IEEJ Journal of Industry Applications
Vol.6 No.6 pp.409–415 DOI: 10.1541/ieejjia.6.409

**Paper**

# Design of Surface Permanent Magnet Synchronous Motor Using Design Assist System for PMSM

Kenta Yamano* Student Member, Shigeo Morimoto*a) Senior Member
Masayuki Sanada* Senior Member, Yukinori Inoue* Member

(Manuscript received Jan. 16, 2017, revised March 30, 2017)

Permanent magnet synchronous motors (PMSMs) possess many good characteristics, such as high efficiency and high torque density. In this study, a design assist system is proposed for PMSMs. This system uses motor parameters and a magnetic equivalent circuit to design a PMSM that satisfies the demanded output characteristics. This paper describes the outline of the design assist system. The system is applied to the design of surface permanent magnet synchronous motors (SPMSMs) and the effectiveness of the proposed system is confirmed.

**Keywords:** SPMSM, motor parameters, magnetic circuit, permeance model

## 1. Introduction

Permanent magnet synchronous motors (PMSMs) are widely used in many applications, such as home applications and electric vehicles. Due to their high efficiency and power density, they contribute to energy savings [(1)(2)].

An optimized motor design must take into account requirements such as the torque-speed characteristics and motor size, because they are different for each application [(3)(4)]. The PMSM design is complex, so engineers must have experience that designed a lot of various motors. However, the motor design typically involves time-consuming trial and errors [(5)–(7)]. Therefore, a design assist system that can automatically decide the motor structure to decrease the trial and error process of the PMSM design is in demanded.

This study proposes a design assist system for PMSM that automatically decides motor structures based on the demanded operating points on output characteristics and required motor size. The proposed system is applied to the design of surface permanent magnet synchronous motor (SPMSM), and two designed models are analyzed by the finite element method (FEM). The effectiveness of the proposed system is discussed by evaluating the results of the analyses.

## 2. Design Assist System for PMSM

A flowchart for the proposed design assist system is shown in Fig. 1. The proposed system determines the motor structure parameters from the motor parameters obtained from the demanded operating points on output characteristics and the restriction of motor size.

The system is divided into two processes: (1) selection of the motor parameters and (2) calculation of the motor structure parameters. First, the motor parameters satisfying the demanded operating points are selected with consideration of the optimal current vector control under the current and voltage limitations. Then, the magnetic equivalent circuit based on the permeance model is used in the calculation of the motor structure parameters by using the motor parameters.

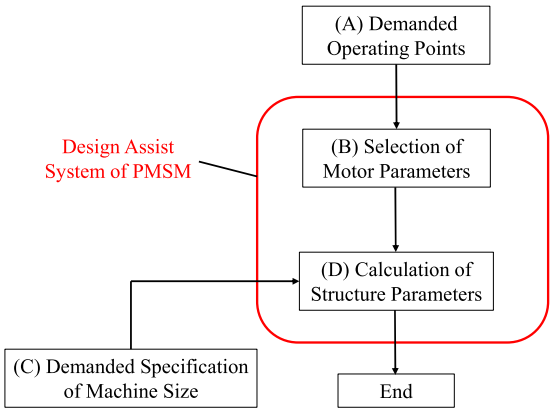



Fig. 1. Flowchart for proposed design assist system

Each process is described in detail in the following.

## 3. Selection of Motor Parameters

The voltage equation and the torque of a surface permanent magnet synchronous motor (SPMSM) modeled in the $d$-$q$ reference frame are expressed as follows:

$$\begin{bmatrix} v_d \\ v_q \end{bmatrix} = \begin{bmatrix} R_a + pL_a & -\omega L_a \\ \omega L_a & R_a + pL_a \end{bmatrix} \begin{bmatrix} i_d \\ i_q \end{bmatrix} + \begin{bmatrix} 0 \\ \omega \Psi_a \end{bmatrix} \quad \cdots\cdots (1)$$

$$T = P_n \Psi_a i_q \quad \cdots\cdots (2)$$

where

$v_d$, $v_q$ $d$- and $q$-axis voltages
$i_d$, $i_q$ $d$- and $q$-axis currents
$R_a$ armature resistance

a) Correspondence to: Shigeo Morimoto. E-mail: morimoto@eis.osakafu-u.ac.jp
* Osaka Prefecture University
1-1, Gakuencho, Naka-ku, Sakai, Osaka 591-8531, Japan

© 2017 The Institute of Electrical Engineers of Japan.

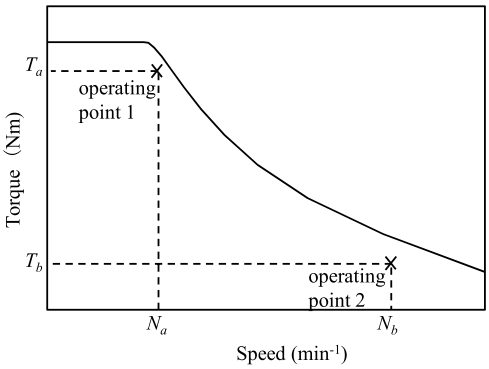



Fig. 2. Example of torque vs. speed characteristics

$L_a$ inductance (corresponding to $d$- and $q$-axis inductances $L_d$, $L_q$)
$\omega$ electrical rotor angular velocity
$p$ differential operator
$P_n$ number of pole pairs

Equations (1) and (2) show that the output characteristics of the SPMSM depend on the motor parameters. Motor parameters are important in the SPMSM design because they decide the torque vs. speed characteristics like Fig. 2. In the proposed design assist system of the SPMSM, motor parameters satisfying the demanded operating points on output characteristics are found and used to design the SPMSM. To find the motor parameters satisfying the demanded output characteristics, this system uses the optimal current vector control method to obtain the maximum output under the current and voltage limitations.

The current and voltage are limited to

$$V_o = \omega\sqrt{(\Psi_a + L_a i_d)^2 + (L_a i_q)^2} \le V_{om} \cdots\cdots (3)$$

$$I_a = \sqrt{{i_d}^2 + {i_q}^2} \le I_{am} \cdots\cdots (4)$$

where

$V_o$ induced voltage
$V_{om}$ induced voltage limit
$I_a$ armature current
$I_{am}$ armature current limit

In the following, the relationships between the motor parameters and the demanded operating points like Fig. 2 are derived under the current vector control methods.

**3.1 Maximum Torque per Ampere Control** Maximum torque per ampere (MTPA) control is applied in the region of speed where the induced voltage $V_o$ does not exceed the induced voltage limit $V_{om}$. In this control region, the armature current $I_a$ is equal to the current limit $I_{am}$, and the induced voltage $V_o$ is less than the voltage limit $V_{om}$. The $d$- and $q$-axis currents in the control region and torque are given as follows:

$$i_{d1} = 0 \cdots\cdots (5)$$

$$i_{q1} = I_{am} \cdots\cdots (6)$$

$$T = P_n \Psi_a I_{am} \cdots\cdots (7)$$

From (7), the magnet flux-linkage $\Psi_a$ is calculated as follows:

$$\Psi_a = \frac{T}{P_n I_{am}} \cdots\cdots (8)$$

From (8) and the demanded maximum torque $T_a$ in Fig. 2, the relationship between $\Psi_a$ and $L_a$ satisfying the demanded maximum torque is obtained.

**3.2 Base Speed** When the induced voltage $V_o$ reaches the voltage limit $V_{om}$ under maximum torque per ampere control, the speed is called base speed $\omega_{base}$. From (3), (5) and (6), the base speed for SPMSM is given as follows:

$$\omega_{base} = \frac{V_{om}}{\sqrt{{\Psi_a}^2 + (L_a I_{am})^2}} \cdots\cdots (9)$$

From (9), the relationship between the motor parameters of $L_a$ and $\Psi_a$ is as follows:

$$L_a = \frac{1}{I_{am}}\sqrt{\left(\frac{V_{om}}{\omega_{base}}\right)^2 - {\Psi_a}^2} \cdots\cdots (10)$$

From (10) and base speed $N_{base}$ (= $N_a$) in Fig. 2, the relationship between $\Psi_a$ and $L_a$ satisfying the demanded base speed is obtained.

**3.3 Flux-weakening Control for Maximizing Torque** Induced voltage increases with increasing rotor speed. When the motor speed reaches the base speed under MTPA control, the induced voltage becomes equal to the induced voltage limit. Therefore, the induced voltage $V_o$ is controlled to the induced voltage limit $V_{om}$ by flux-weakening (FW) control above the base speed. In this control region, voltage and current are equal to their limiting values. The $d$- and $q$-axis currents in this control region are given as follows:

$$i_{d2} = \frac{\left(\frac{V_{om}}{\omega}\right)^2 - {\Psi_a}^2 - {L_d}^2 {I_{am}}^2}{2L_a\Psi_a} \cdots\cdots (11)$$

$$i_{q2} = \sqrt{{I_{am}}^2 - {i_{d2}}^2} \cdots\cdots (12)$$

From (2), (11) and (12), the relationship between the motor parameters is as follows:

$$L_a = \frac{P_n\sqrt{A({\Psi_a}^2 + B^2) - 2(T^2 + \sqrt{C - D})}}{A} \cdots\cdots (13)$$

where

$A = {P_n}^2 {I_{am}}^2$
$B = V_{om}/\omega$
$C = (T^2 + AB\Psi_a)^2$
$D = AT^2(B + \Psi_a)^2$

From (13) and the torque and speed at the demanded high speed operating point, such as operating point 2 ($T_b$ and $N_b$) in Fig. 2, the relationship between $\Psi_a$ and $L_a$ satisfying the demanded operating point is obtained.

**3.4 Maximum Torque per Voltage Control** If $\Psi_{d\min}$ (= $\Psi_a - L_a I_{am}$) < 0, maximum torque can be obtained in the high-speed flux-weakening region by applying maximum torque per voltage (MTPV) control. In this control region, induced voltage $V_o$ is equal to voltage limit $V_{om}$ and armature current $I_a$ is less than current limit $I_{am}$. The $d$- and $q$-axis currents in this control region are given as follows:

$$i_{d3} = -\frac{\Psi_a}{L_a} \cdots\cdots (14)$$

$$i_{q3} = \frac{V_{om}}{\omega L_a} \cdots\cdots (15)$$

Table 1. Operating points and electrical specification

| Item (Unit) | | Value |
|---|---|---|
| Operating point 1 | Speed $N_a$ (min$^{-1}$) | 1500 |
| | Torque $T_a$ (Nm) | 10 |
| Operating point 2 | Speed $N_b$ (min$^{-1}$) | 3000 |
| | Torque $T_b$ (Nm) | 5 |
| Armature current limit $I_{am}$ (A) | | 20 |
| Induced voltage limit $V_{om}$ (V) | | 100 |
| Voltage limit of inverter $V_{\lim}$ (V) | | 160 |

From (2), (14) and (15), the relationship between motor parameters is as follows:

$$L_a = \frac{P_n V_{om} \Psi_a}{\omega T} \cdots\cdots (16)$$

From (16) and torque and speed like $T_b$ and $N_b$ in Fig. 2, the relationship between $\Psi_a$ and $L_a$ satisfying the demanded operating point is obtained.

**3.5 Voltage Limit of Inverter** The SPMSM is usually driven by an inverter. In the high speed region, the induced voltage $V_o$ is controlled under the induced voltage limit $V_{om}$ by flux-weakening control. However, the back electromotive force due to the permanent magnet can no longer be controlled when the uncontrolled generator mode occurs as a result of inverter shutdown at high speeds. To drive the SPMSM safely, the induced voltage under the no-load state must not exceed the voltage limit of inverter $V_{\lim}$. The voltage limit $V_{\lim}$ corresponds to the voltage on the *d-q* coordinate converted from the withstand voltage of the inverter (limit value of the DC link voltage) which is determined by the withstand voltage of power device and the breakdown voltage of the smoothing capacitor. In the proposed system, it is considered that no-load induced voltage doesn't exceed $V_{\lim}$. This condition is expressed as follows:

$$V_{\lim} = \omega \Psi_a \cdots\cdots (17)$$

From (17), magnet flux-linkage $\Psi_a$ is as follows:

$$\Psi_a = \frac{V_{\lim}}{\omega} \cdots\cdots (18)$$

From (18) and maximum operating speed like $N_b$ in Fig. 2, the maximum value of $\Psi_a$ satisfying the voltage limit of the inverter is obtained.

**3.6 Design of Motor Parameters** The demanded operating points and limiting values discussed in this paper are shown in Table 1. In this paper, the voltage limit of inverter $V_{\lim}$ was set to 160 V as shown in Table 1. Generally, the induced voltage limit $V_{om}$ determined by the DC link voltage during normal operation is set lower than $V_{\lim}$ in consideration of the safety factor, so it was set to 100 V in this paper.

In the design of the SPMSM, motor parameters satisfying two demanded operating points under the limitations of current and voltage are obtained from (8), (10), (13), (16), (18) and Table 1. The motor parameters region is shown in Fig. 3. In Fig. 3, border 1 is obtained from (8) and $T_a$ in Table 1. The right side of border 1 shows the motor parameters satisfying the maximum torque $T_a$. Border 2 is obtained from (10) and $N_a$ in Table 1. The lower side of border 2 shows

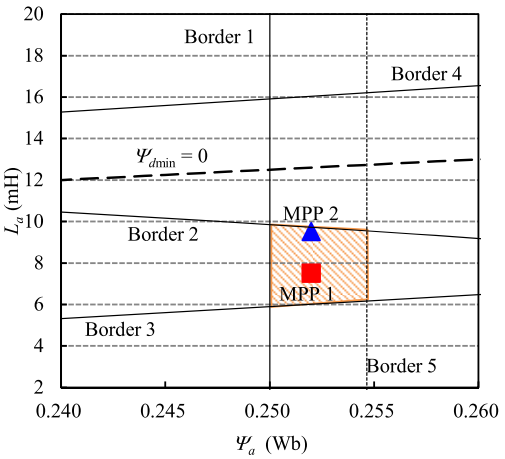



Fig. 3. Motor parameters region

Table 2. Values of MPP 1 and MPP 2

| Item (Unit) | Value | |
|---|---|---|
| Selected motor parameters | MPP 1 | MPP 2 |
| Magnet flux-linkage $\Psi_a$ (Wb) | 0.252 | 0.252 |
| Inductance $L_a$ (mH) | 7.5 | 9.5 |

the motor parameters satisfying the base speed of $N_a$. Border 3 is obtained from (13) and $T_b$ and $N_b$ in Table 1. The upper side of border 3 shows the motor parameters satisfying $T_b$ and $N_b$. Border 4 is obtained from (16) and $T_b$ and $N_b$ in Table 1. The lower side of border 4 shows the motor parameters satisfying $T_b$ and $N_b$. Finally, border 5 is obtained from (18) and $N_b$ in Table 1. The left side of border 5 shows the motor parameters satisfying the voltage limit of the inverter at $N_b$. Therefore, the motor parameters satisfying the conditions listed in Table 1 exist within the region enclosed by borders 1, 2, 3, 4 and 5, which correspond to the hatched area in Fig. 3. This area can be theoretically obtained based on the theory described in 3.1 to 3.5 without the experience or skill of the designer.

In this design, motor parameter points 1 and 2 (MPP 1, MPP 2) in Fig. 3 are selected. The values of MPP 1 and 2 are shown in Table 2. If the motor parameters near each border was selected, the margin for the demanded operating points decreases. In consideration of margin, MPP 1 was selected as the design point near the center of the hatched area in Fig. 3. On the other hand, it is known that the decrease of torque at high speed becomes small when the combination of motor parameters close to the line representing $\Psi_{d\min} = 0$ are selected. The motor parameter point MPP 2 was selected to confirm that.

The torque versus speed characteristics calculated by using the motor parameters at MPP 1 and 2 are shown in Fig. 4. Figure 4 shows that SPMSMs with motor parameters selected by Fig. 3 satisfy the demanded operating points 1 and 2 shown in Table 1. Therefore, the motor parameters at MPP 1 and 2 are used for the design of SPMSMs that satisfy the demanded specifications of Table 1. Figure 4 also shows that the torque at high speed for MPP2 is larger.

## 4. Calculation of Motor Structure Parameters

The diagram of the calculation of the motor structure

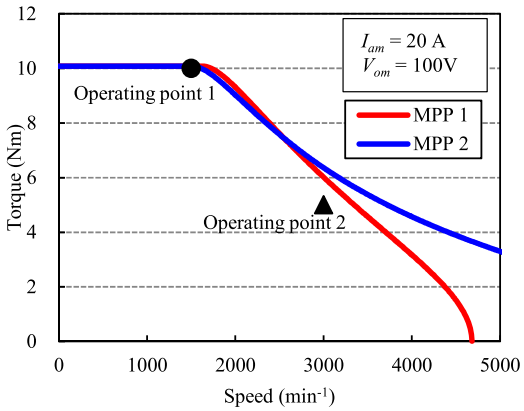



Fig. 4. Torque vs. speed characteristics calculated using motor parameters at MPP 1 and 2

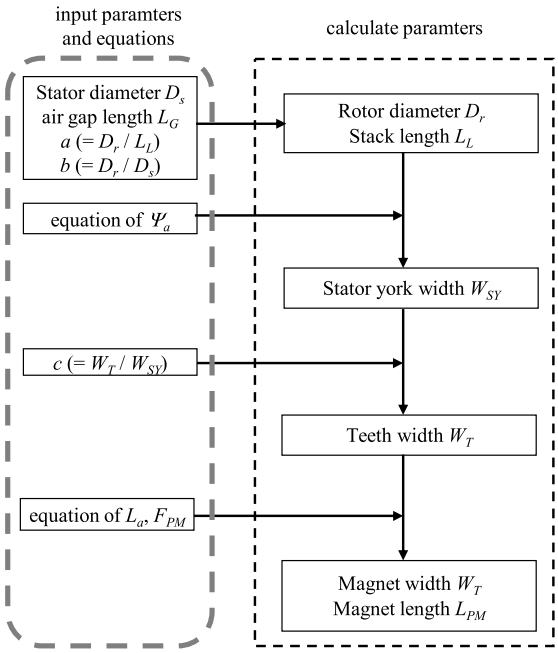


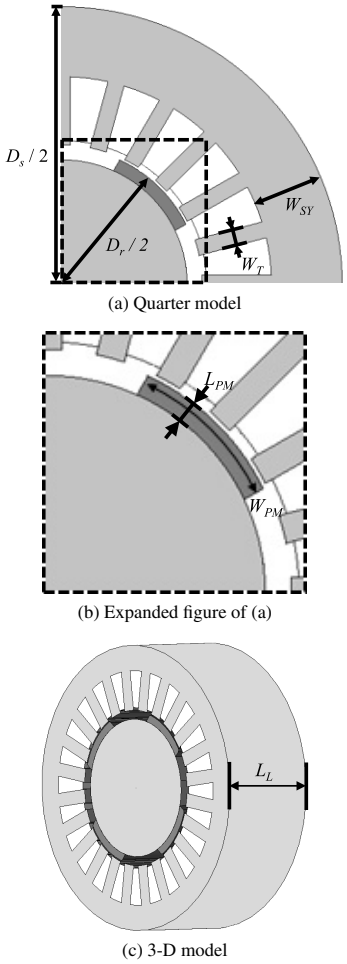

Fig. 5. Method of SPMSM design

parameters is shown in Fig. 5. In this method, motor structure parameters are obtained from motor parameters such as $\Psi_a$ and $L_a$. To obtain the motor structure parameters from motor parameters, this system uses a simple magnetic equivalent circuit based on the permeance model.

**4.1 Permeance Model** An example of the design model and the motor structure parameters is shown in Fig. 6. The model is SPMSM which is a four-pole SPMSM with distributed winding stator with 24 slots. Using the design system, $D_r$, $L_L$, $W_{SY}$, $W_T$, $L_{PM}$ and $W_{PM}$ are calculated.

The magnetic equivalent circuit considered in this system is shown in Fig. 7 and a list of reluctances is shown in Table 3. In Fig. 7, the numbers of reluctances and motor structure parameters are set as small as possible in order to calculate the structure parameters. In the following, relationship between the motor structure parameters and the motor parameters is shown using the magnetic equivalent circuit.

**4.2 Magnet Flux-Linkage** Magnet flux-linkage $\Psi_a$ can be calculated by magnetic flux $\phi$ and coil turns per phase $N_c$ as follows:




(a) Quarter model

(b) Expanded figure of (a)

(c) 3-D model

Fig. 6. Structure of SPMSM

Table 3. List of reluctances

| Item | Symbol |
|---|---|
| Stator yoke | $R_{SY}$ |
| Teeth | $R_T$ |
| Air gap between teeth and magnet | $R_{G1}$ |
| Permanent magnet | $R_{PM}$ |
| Air gap both sides of magnet | $R_{G2}$ |
| Rotor yoke | $R_{RY}$ |

$$\Psi_a = \sqrt{\frac{3}{2}} N_c \phi \cdots\cdots (19)$$

To use (19), magnetic flux $\phi$ and coil turns per phase $N_c$ are as follows:

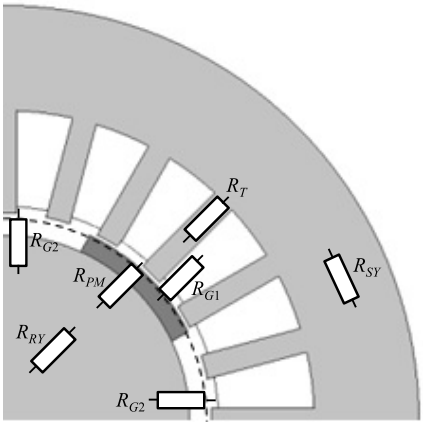
$$\phi = B_{SY} S_{SY} \cdots\cdots (20)$$

$$N_c = \frac{4uS_{slot}N_{slot}}{6S_{wire}} \cdots\cdots (21)$$

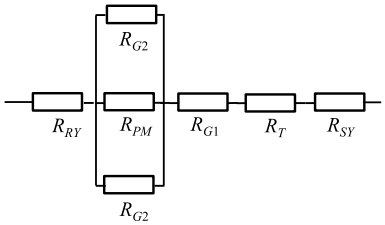
where

$B_{SY}$ magnetic flux density of stator yoke
$S_{SY}$ area of stator yoke ( = $W_{SY}$ $L_L$)
$u$ winding space factor
$S_{slot}$ area of slot
$S_{wire}$ area of conducting wire
$N_{slot}$ number of slot

Using (19), (20), (21), and stack length $L_L$, stator yoke




(a) Reluctance.




(b) $d$, $q$-axis combined reluctances.

Fig. 7. Magnetic equivalent circuit

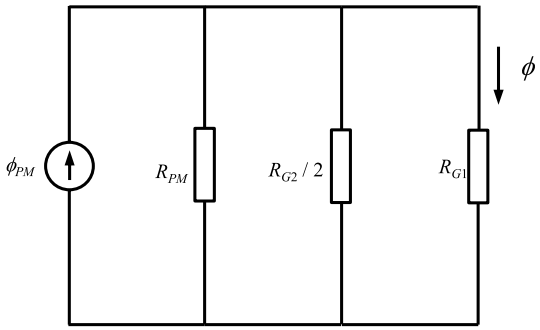



Fig. 8. Magnetic circuit from permeance model

width $W_{SY}$ is calculated. Here, magnet flux-linkage $\Psi_a$ given from the selection of motor parameters is used.

**4.3 Inductance** From Fig. 7, the sum of $d$-axis reluctance $R_d$ is obtained as follows:

$$R_d = R_{SY} + R_T + R_{G1} + R_{PMG2} + R_{RY} \cdots\cdots\cdots\cdots (22)$$

where

$$R_{PMG2} = R_{PM}R_{G2}/(2R_{PM} + R_{G1})$$

From (22), $d$-axis inductance $L_a$ is as follows:

$$L_a = \frac{3{N_c}^2}{8R_d} \cdots\cdots\cdots\cdots\cdots\cdots\cdots\cdots\cdots\cdots\cdots\cdots (23)$$

**4.4 Magnetomotive Force** The magnetic circuit from permanent magnet is shown in Fig. 8. In Fig. 8, only reluctances of $R_{G1}$, $R_{G2}$ and $R_{PM}$ are considered in order to constitute a simplified magnetic circuit. From Fig. 8, the equation of magnet flux $\phi_{PM}$ is given as follows:

$$\begin{aligned}\phi_{PM} &= \phi\left(\frac{1}{R_{PM}} + \frac{1}{R_{G1}} + \frac{1}{R_{G2}}\right) \div \frac{1}{R_{G1}} \\ &= B_{SY}S_{SY}\left(\frac{1}{R_{PM}} + \frac{1}{R_{G1}} + \frac{1}{R_{G2}}\right) \times R_{G1} \cdots\cdots (24)\end{aligned}$$

Table 4. Parameters decided by motor designer

| Item (Unit) | Value |
|---|---|
| Stator diameter $D_s$ (mm) | 124 |
| Air gap length $L_{G1}$ (mm) | 1.0 |
| Numbers of teeth $N_t$ | 24 |
| Cross-sectional area of the conducting wire $S_{wire}$ (mm$^2$) | 0.632 |
| Space factor $u$ | 0.5 |
| Relative permeability of electrical sheet $\mu_s$ | 1000 |
| Magnetic flux density of stator yoke $B_{SY}$ (T) | 0.85 |
| $a$ (= $D_r$ / $L_L$) | 1.5 |
| $b$ (= $D_r$ / $D_s$) | 0.5 |
| $c$ (= $W_T$ / $W_{SY}$) | 0.5 |
| Coercive force $H_{cb}$(kA / m) | 900 |

Table 5. Result of structure parameters

| Item (Unit) | Value | |
|---|---|---|
| Model | SPM-1 | SPM-2 |
| Selected motor parameters | MPP 1 | MPP 2 |
| Stator diameter $D_s$ (mm) | 124 | |
| Airgap length $L_G$ (mm) | 1.0 | |
| Rotor diameter $D_r$ (mm) | 62 | |
| Stack length $L_L$ (mm) | 41.3 | |
| Stator york width $W_{SY}$ (mm) | 12.8 | |
| Teeth width $W_T$ (mm) | 6.4 | |
| Magnet length $L_{PM}$ (mm) | 5.23 | 3.85 |
| Magnet width $W_{PM}$ (mm) | 23.96 | 25.63 |

By using (24), the magnetomotive force $F_{PM}$ is as follows:

$$F_{PM} = R_{PM}\phi_{PM} \cdots\cdots\cdots\cdots\cdots\cdots\cdots\cdots\cdots\cdots (25)$$

By using the magnet coercive force $H_{cb}$, magnetomotive force $F_{PM}$ is also given as follows:

$$F_{PM} = H_{cb}L_{PM} \cdots\cdots\cdots\cdots\cdots\cdots\cdots\cdots\cdots\cdots (26)$$

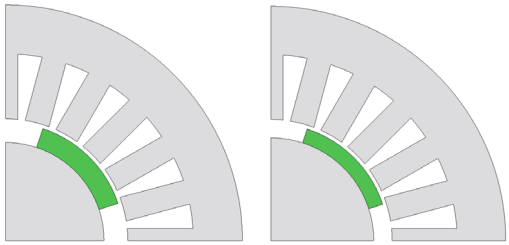
From (25) and (26), the following equation is obtained:

$$R_{PM}\phi_{PM} = H_{cb}L_{PM} \cdots\cdots\cdots\cdots\cdots\cdots\cdots\cdots\cdots\cdots (27)$$

From (23), (27) and $R_{PM} = L_{PM}/\mu_0 W_{PM}L_L$, magnet length $L_{PM}$ and magnet width $W_{PM}$ are obtained. The calculation of magnet length $L_{PM}$ and magnet width $W_{PM}$ uses $d$-axis inductance $L_d$ obtained from the selection of motor parameters.

**4.5 Design of Motor Structure Parameters** The motor parameters in this design are shown in Table 4. The motor parameters are decided by a designer who design SPMSM by using the design assist system and the demanded specifications in advance. The values of the parameters in Table 4 are used. Generally, it is considered that the following dimensional ratios are suitable in the design of a high efficient motor [8][9]. The ratio $a$ (= $D_r/L_L$) is about 1.5. The ratio $b$ (= $D_r/D_s$) is about 0.5 to 0.6. The ratio $c$ (= $W_T/W_{SY}$) is about 0.5 to 0.6. In this paper, each value was selected within the above-mentioned suitable range.

The designed results are shown in Table 5. Two designed



(a) SPM-1. (b) SPM-2.

Fig. 9. Designed models

Table 6. Analysis condition

| Item (Unit) | Value or Grade |
|---|---|
| Armature current limit $I_{am}$ (A) | 20 |
| Induced voltage limit $V_{om}$ (V) | 100 |
| Electrical steel sheet | 50H470 |
| Magnet | NMX-39EH (60°C) |
| Number of elements in mesh | about 23000 |

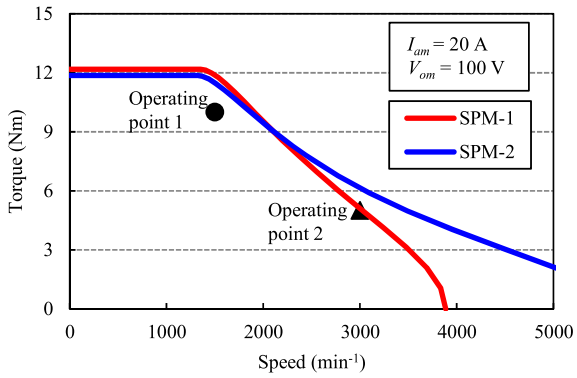



Fig. 10. Torque vs. speed characteristics of designed models

models are shown in Fig. 9. In the proposed design method, $\Psi_a$ given by (19) is mainly used for stator design and $L_a$ given by (23) is mainly used for rotor design. Therefore, the same stator was designed in SPM-1 and SPM-2 because $\Psi_a$ is the same as shown in Table 2. On the other hand, the smaller the distance between the stator inner diameter and the rotor core outer diameter, the smaller the reluctance $R_d$, and as a result $L_a$ increases. Therefore, it is thought that the magnet length of SPM-2 designed based on MPP-2 with larger $L_a$ became smaller than that of SPM-1 designed based on MPP-1 with smaller $L_a$.

## 5. Analysis Result of Designed Model

To confirm that the designed models satisfy the demanded output characteristics, these models are analyzed by 2-D finite element method (FEM). The analysis condition is shown in Table 6. The torque-speed characteristics for the designed models are shown in Fig. 10. In Fig. 10, it is shown that the models satisfy the demanded output characteristics.

The values of magnet flux-linkage $\Psi_a$ and inductance $L_a$ of the designed motors, which were calculated by FEM, together with the selected motor parameters (the same values in Table 2) are shown in Table 7. The parameters of the designed motor are 10 to 20% larger than the selected motor parameters. The reason for this is that the calculation of motor structure parameters proposed in this paper is based on a simple magnetic equivalent circuit, the values of $\mu_s$ and $B_{SY}$ used in designing were maybe different from the values of the designed motor. The appropriate setting of these parameters is a future task.

Table 7. Selected motor parameters and designed motor parameters

| Item (Unit) | MPP-1 | SPM-1 | MPP-2 | SPM-2 |
|---|---|---|---|---|
| $\Psi_a$ (Wb) | 0.252 | 0.304 | 0.252 | 0.297 |
| $L_a$ (mH) | 7.5 | 8.92 | 9.5 | 10.4 |

The characteristics of Figs. 10 and 4 appear to be somewhat different. The reason for this is that the parameters of the designed motor are different from the selected motor parameters as shown in Table 7. In the designed motor, the maximum torque was increased due to the increase in $\Psi_a$, and the torque at high speeds (in the flux-weakening control region) became lower as $\Psi_a$ and $L_a$ increased.

## 6. Conclusions

This paper proposes and describes a design assist system of the PMSM. This proposed system uses motor parameters that satisfy the demanded output characteristics, and is applied to the design of SPMSM. The motor structure parameters are calculated from the motor parameters and the restriction of motor size by using the magnetic equivalent circuit. The results of 2-D FEM analyses confirm that the SPMSMs designed by the proposed system satisfy the demanded output characteristics and the motor size. Therefore, the effectiveness of this proposed system is shown.

**Acknowledgment**

This work was supported by JSPS KAKENHI Grant Number JP23560335.

## References

( 1 ) S. Morimoto, Y. Asano, T, Kosaka, and Y. Enomoto: “Recent Technical Trends in PMSM”, in Proc. IPEC-2014, pp.1997–2003 (2014)

( 2 ) G. Peelegrino, A. Vagati, and P. Guglielmi: “Design Tradeoffs Between Constant Power Speed Range, Uncontrolled Generator Operation, and Rated Current of IPM Motor Drives”, *IEEE Trans. Ind. Appl.*, Vol.47, No.5, pp.1995–2003 (2011)

( 3 ) N. Bernard, F. Martin, and M. E. Zaim: “Design Methology of a Permanent Magnet Synchronous Machine for a Screwdriver Application”, *IEEE Trans. Energy. Conver.*, Vol.27, No.3, pp.624–633 (2012)

( 4 ) T. Yamada and K. Akatsu: “Automatic Design Method Considering the Frequently Used Area of a PMSM for an HEV”, in Proc. ICEMS-2012 (2012)

( 5 ) N. Limsuwan, T. Fukushige, K. Akatsu, and R.D. Lorenz: “Design Methodology for Variable-Flux, Flux-Intensifying Interior Permanent Magnet Machines for an Electric-Vehicle-Class Inverter Rating”, in Proc. ECCE-2013, pp.1547–1554 (2013)

( 6 ) B. Boazzo, G. Pellegrino, and A. Vagati: “Multipolar SPM Machines for Direct-Drive Application: A General Design Approach”, *IEEE Trans. Ind. Appl.*, Vol.50, No.1, pp.327–337 (2014)

( 7 ) H.W. Lee, K.D. Lee, W.H. Kim, I.S. Jang, M.J. Kim, J.J. Lee, and J. Lee: “Parameters Design of IPMSM With Concentrated Winding Considering Partial Magnetic Saturation”, *IEEE Trans. Magn.*, Vol.47, No.10, pp.3653–3656 (2011)

( 8 ) JMAG motor design study group: “Introduction to Permanent Magnet Synchronous Motor Design”, JSOL Corp. (2015) (in Japanese)

( 9 ) X. Ning, M. Sanada, and S. Morimoto: “Investigation of Design Parameters on Permanent Magnet Motors for HEV Applications”, in Proc. ICEMS-2009, DS2G06_05 (2009)

**Kenta Yamano** (Student Member) received the B.E. and M.E. degrees from Osaka Prefecture University, Sakai, Japan, in 2015 and 2017, respectively. He was involved in the study on the design of permanent magnet synchronous motors at Osaka Prefecture University. He is currently with OBAYASHI CORPORATION, Tokyo, Japan.



**Shigeo Morimoto** (Senior Member) received the B.E., M.E., and Ph.D. degrees from Osaka Prefecture University, Sakai, Japan, in 1982, 1984, and 1990, respectively. In 1984, he joined Mitsubishi Electric Corporation, Tokyo, Japan. Since 1988, he has been with the Graduate School of Engineering, Osaka Prefecture University, where he is currently a Professor. His main areas of research interest are permanent magnet synchronous machines, reluctance machines and their control systems. Dr. Morimoto is a member of the IEEE, the Society of Instrument and Control Engineers of Japan, the Institute of Systems, Control and Information Engineers, and the Japan Institute of Power Electronics.



**Masayuki Sanada** (Senior Member) received the B.E., M.E., and Ph.D. degrees from Osaka Prefecture University, Sakai, Japan, in 1989, 1991, and 1994, respectively. Since 1994, he has been with the Graduate School of Engineering, Osaka Prefecture University, where he is currently an Associate Professor. His main areas of research interest are permanent-magnet motors for direct-drive applications, their control systems, and magnetic field analysis. Dr. Sanada is a member of the IEEE, the Japan Institute of Power Electronics, and the Japan Society of Applied Electromagnetics and Mechanics.



**Yukinori Inoue** (Member) received the B.E., M.E., and Ph.D. degrees from Osaka Prefecture University, Sakai, Japan, in 2005, 2007, and 2010, respectively. Since 2010, he has been with the Graduate School of Engineering, Osaka Prefecture University, where he is currently an Associate Professor. His research interests include control of electrical drives, in particular, the direct torque control of permanent magnet synchronous motors and position sensorless control of these motors. Dr. Inoue is a member of the IEEE and the Japan Institute of Power Electronics.

